JOURNAL OF COMPUTATIONAL PHYSICS 100, 200–204 (1992)

NOTE

A Fixed-Stencil Non-oscillatory Scheme for Hyperbolic Systems

1. INTRODUCTION

Following the ground-breaking work of Harten [1], several TVD schemes have been successfully formulated and widely used by the CFD community [2–5]. TVD schemes are monotonicity preserving and produce oscillation-free solutions for hyperbolic systems. In order to diminish the total variation of the solution, TVD schemes automatically reduce to first-order spatial differencing at local solution extrema. Away from local extrema, TVD schemes can be of high-order accuracy. This reduction of accuracy at local extrema restricts the global error of TVD schemes to only first-order in L_∞ norm. This is an undesirable property of TVD schemes, particularly when applied to problems with periodic transient waves or vortical flows. To remedy this shortcoming, Harten and Osher [6, 7] introduced their "uniformly high-order accurate essentially non-oscillatory schemes" (UNO or ENO) for hyperbolic systems. These schemes are non-oscillatory in the sense that while the total variation of the solution is allowed to increase in a bounded fashion, the number of solution extrema is not increasing. UNO schemes are still monotonicity preserving and are uniformly of high-order accuracy even at local extrema. To achieve the non-oscillatory property, a Kth-order UNO scheme uses an interpolation polynomial that is the "smoothest" one among K different possible choices. Thus, the stencil of UNO schemes is adaptive and can spread over $2K+1$ grid points for a Kth-order scheme. Comparing with the fixed-stencil TVD schemes, UNO schemes higher than second-order are arithmetically more complex and computationally more expensive.

It was intended to find a simple way to increase the accuracy of TVD schemes at local solution extrema. This must be done in a non-oscillatory fashion to prevent Gibb's oscillation around discontinuities. The basic scheme used here is the five-point fixed-stencil scheme of Chakravarthy and Osher [2], which can be third-order accurate (TVD3) for linear model problems. To maintain at least second-order accuracy at solution extrema, a limiter based on the second-order UNO formulation (UNO2) is constructed to replace the TVD limiter. The new limiter is used for three purposes: (1) to bound the total variation of the solution, (2) to distinguish between smooth extrema and discontinuities, and (3) to restrict the stencil to only five points. This results in a fixed-stencil non-oscillatory scheme, which can be third-order accurate for linear model problems. Hence, it is designated as FNO3.

2. FORMULATIONS

Consider a system of hyperbolic conservation laws in one spatial dimension (x) and time (t):

$$q_t + f_x = 0. \tag{1}$$

Here, q and f are m-vectors, with q being the set of conservative variables, and f the corresponding flux vector. For hyperbolic equations, the Jacobian matrix $\partial f/\partial q$ has a complete set of linearly independent eigenvectors and real eigenvalues. Consider the conservation law for a cell j, defined by $x_{j-1/2} \leqslant x \leqslant x_{j+1/2}$, the semi-discrete approximation of Eq. (1) can be written as

$$(q_j)_t + \frac{1}{\Delta x}(\hat{f}_{j+1/2} - \hat{f}_{j-1/2}) = 0, \tag{2}$$

where q_j now represents the cell-average of q in cell j; $\hat{f}_{j\pm 1/2}$ are the numerical fluxes at the bounding surfaces of cell j. The MUSCL [8] type schemes use a Riemann solver at each cell interface to evaluate the numerical flux based on the left and right states of the dependent variables q at the cell interface. Assuming that an exact or a "good" approximate Riemann solver is used, it is the construction of the left and right states that dictates the accuracy and the TVD or UNO properties of the scheme. For every time step, the left and right states are constructed to a desired degree of accuracy using piecewise polynomial interpolation of discrete data related to the cell-average q_j. The chosen Riemann solver is then employed to evaluate the numerical flux at each cell interface. With a suitable time discretization, the overall algorithm should be stable, and TVD or UNO according to the properties of the interpolation polynomial. Assuming that the cell-average data $\{q_j\}$ are available at the cell centroids $\{x_j\}$, and let $\Delta_{j+1/2} q = q_{j+1} - q_j$. Following Chakravarthy and Osher [2], the

0021-9991/92 $5.00

formulae for the left "−" and right "+" states at the cell interface can be given by

$$q^{-}_{j+1/2} = q_j + \left\{ \frac{1+\phi}{4} \widetilde{\Delta_{j+1/2} q} + \frac{1-\phi}{4} \widehat{\Delta_{j-1/2} q} \right\}$$
$$q^{+}_{j-1/2} = q_j - \left\{ \frac{1+\phi}{4} \widehat{\Delta_{j-1/2} q} + \frac{1-\phi}{4} \widetilde{\Delta_{j+1/2} q} \right\}, \quad (3)$$

where $\widetilde{\Delta_{j\pm1/2} q}$ and $\widehat{\Delta_{j\pm1/2} q}$ are the slope-limited values of $\Delta_{j\pm1/2} q$. The parameter ϕ can be chosen between -1 and $+1$ to vary the truncation error of the scheme. Of specific interest here is that the scheme is third-order accurate for $\phi = \frac{1}{3}$. The "minmod" operator and the FNO3 limiter is given as

$$\text{minmod}\{x, y\} = \begin{cases} s \cdot \min(|x|, |y|), & \text{if } \operatorname{sgn}(x) = \operatorname{sgn}(y) = s, \\ 0, & \text{otherwise;} \end{cases}$$

$$\operatorname{sgn}(x) = \begin{cases} x/|x|, & \text{if } x \neq 0, \\ 0, & \text{if } x = 0; \end{cases}$$

$$D_j q = \Delta_{j+1/2} q - \Delta_{j-1/2} q$$

$$D_{j+1/2} q = \text{minmod}\{D_j q, D_{j+1} q\}$$

$$S_j = \text{minmod}\{(\Delta_{j+1/2} q - \tfrac{1}{2} D_{j+1/2} q), (\Delta_{j-1/2} q + \tfrac{1}{2} D_{j-1/2} q)\}$$

if

$$\Delta_{j+1/2} q \cdot \Delta_{j-1/2} q > 0,$$

$$\begin{cases} b^{\pm} = \max\left\{2, \dfrac{S_j}{\Delta_{j\pm1/2} q}\right\}, \qquad \beta^{\pm} = \dfrac{2b^{\pm} - 1 - \phi}{1 - \phi} \\ \widetilde{\Delta_{j+1/2} q} = \operatorname{sgn}(\Delta_{j+1/2} q) \min\{|\Delta_{j+1/2} q|, \beta^{-} |\Delta_{j-1/2} q|\} \\ \widehat{\Delta_{j-1/2} q} = \operatorname{sgn}(\Delta_{j-1/2} q) \min\{|\Delta_{j-1/2} q|, \beta^{+} |\Delta_{j+1/2} q|\} \end{cases}$$

if

$$\Delta_{j+1/2} q \cdot \Delta_{j-1/2} q \leqslant 0,$$

$$\begin{cases} \beta = \max\left\{\dfrac{2}{1+\phi}, \dfrac{2}{1-\phi}\right\} \\ \widetilde{\Delta_{j+1/2} q} = \operatorname{sgn}(\Delta_{j+1/2} q) \min\{|\Delta_{j+1/2} q|, \beta |S_j|\} \\ \widehat{\Delta_{j-1/2} q} = \operatorname{sgn}(\Delta_{j-1/2} q) \min\{|\Delta_{j-1/2} q|, \beta |S_j|\}. \end{cases}$$

In the above limiter, the variation increase is bounded by the UNO2 slope S_j. The parameter ϕ should be greater than or equal to zero to prevent the number of extrema from increasing. By taking $\phi = \frac{1}{3}$, the scheme is globally third-order accurate and is at least second-order in L_∞ norm for linear model problems.

3. TEST RESULTS AND CONCLUSIONS

Due to the limited space of this paper, only part of the test results will be presented. For the sake of comparison, some TVD3 and UNO2 results will also be shown. The first test is the linear scalar wave propagation of continuous and discontinuous functions. The flux function is $f = q$, and the domain is $-1 \leqslant x \leqslant 1$ with periodic boundary conditions. The fourth-order Runge–Kutta (RK4) with a CFL number of 0.8 was used for time marching. For a smooth initial function $q(x, 0) = \sin(2\pi x)$, Figures 1a and b show the comparison of results at $t = 1$. The superior accuracy of the FNO3 scheme over TVD3 and UNO2 can be easily seen. Figures 2a and b show the L_1 and L_∞ norm versus the number of grid points N (or $1/\Delta x$) in the log scale. A second-order curve in the symbol Δ is included for reference use. Note that FNO3 is third-order and UNO2 is second-order for both norms. But TVD3 is only second-order in L_1 norm, although formally it is a third-order scheme. TVD3 drops to

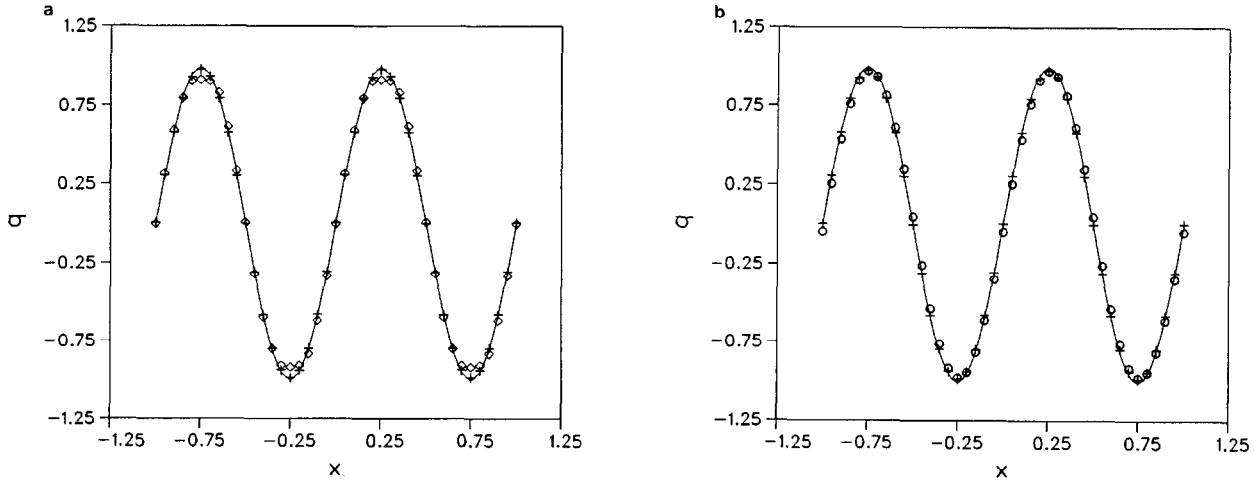

FIG. 1. Linear scalar wave equation, $q(x, 0) = \sin(2\pi x)$, $t = 1$, $N = 40$, CFL = 0.8: (a) −, exact; ◇, TVD3; +, FNO3; (b) −, exact; ○, UNO2, +, FNO3.

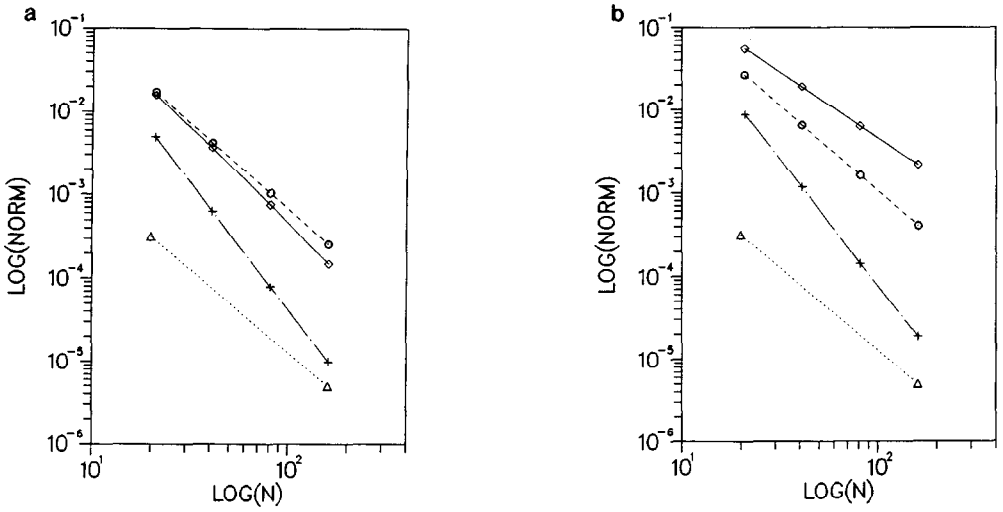

FIG. 2. Norms of Fig. 1: ◇, TVD3; ○, UNO2; +, FNO3; △, 2nd-order curve. (a) L_1 norm; (b) L_∞ norm.

first-order in L_∞ norm. Figures 3a and b are the propagation of a discontinuous profile used in [6]. Again, the FNO3 scheme gives better results than others, especially around the extremum points of the profile.

The second test presented here is the one-dimensional Euler equations with $q=[\rho, \rho u, e]^T$, $f=[\rho u, \rho u^2+p, (e+p)u]^T$, and $p=(\gamma-1)(e-\frac{1}{2}\rho u^2)$. The FNO3 interpolation is done on the characteristic variables to evaluate the cell interface values. Roe's approximate Riemann solver is used for flux calculation. RK4 is used for time integration. The first test is a shock tube problem with the initial right state $(\rho_R, u_R, p_R)=(1., 0., 0.714)$ and left state $(\rho_L, u_L, p_L)=(1., 0., 4p_R)$. The CFL number is 0.8. Figures 4a, b, and c show the density profiles by three schemes at $t=0.25$. It is seen that UNO2 is the most dissipative scheme across the shock and contact discontinuity. FNO3 produces a slight variation increase across the contact discontinuity. This is not unexpected since the TVD requirement was relaxed. The computed density is 1.857 at the right side of contact discontinuity while analytically it is 1.85. This increase is minimal and considered acceptable. The second test problem is the interaction of blast waves suggested by Woodward and Colella [9]. Figures 5a, b, and c show the density plots at $t=0.038$ using 200 cells and CFL number 0.2. The results obtained by a total variation bounded (TVB) method [10] using 1600 cells is shown for comparison. All three schemes capture shocks at around $x=0.65$ and $x=0.86$ within 2 to 3 cells. Because the 200 cells used is less than adequate, all three schemes show similar smearing around contact surfaces at $x=0.6$, $x=0.78$, and $x=0.8$. Nevertheless, FNO3 is the most accurate scheme among them, especially in the vicinity of

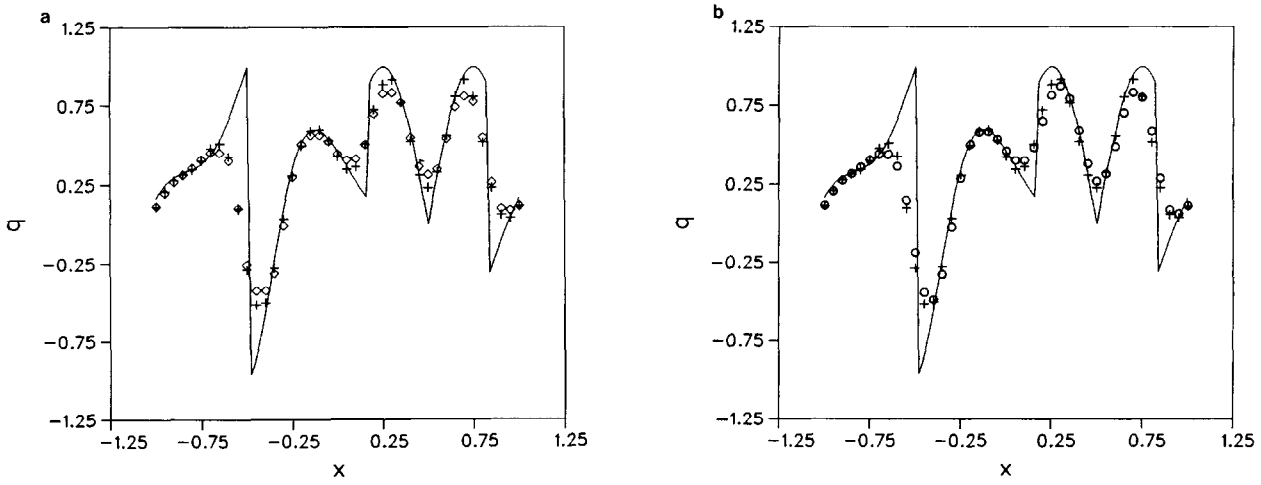

FIG. 3. Linear scalar wave equation, Ref. [6], $t=0.5$, $N=40$, CFL $=0.8$: (a) −, exact; ◇, TVD3; +, FNO3; (b) −, exact; ○, UNO2; +, FNO3.

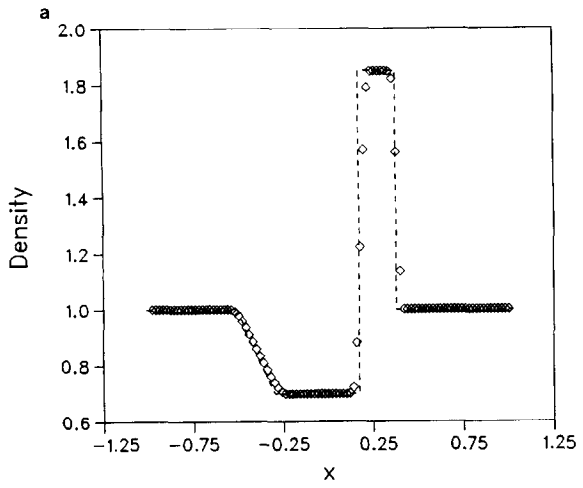

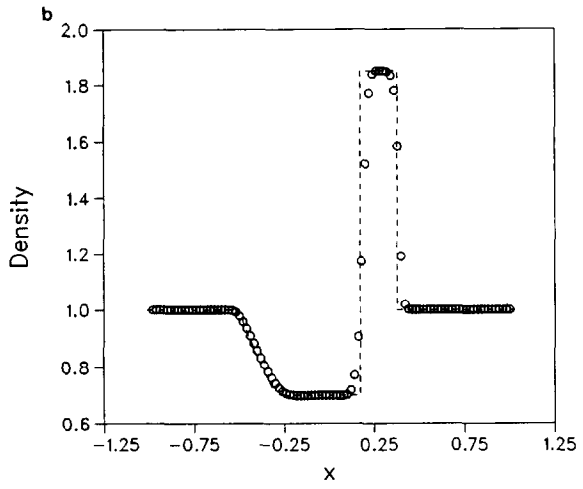

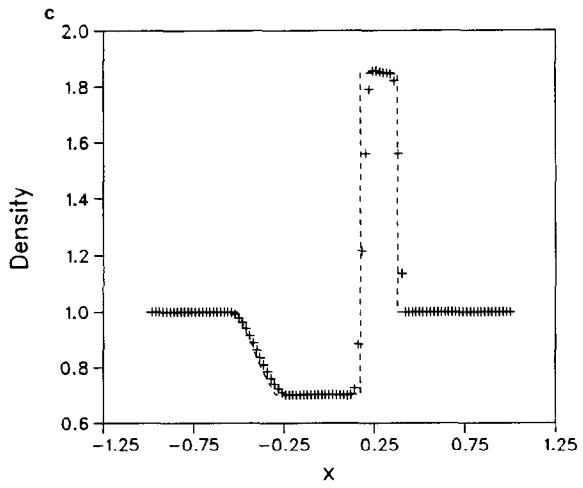

FIG. 4. Shock tube problem, $t = 0.25$, $N = 100$, CFL = 0.8; (a) -, xact; ◇, TVD3; (b) −, exact; ○, UNO2; (c) −, exact; +, FNO3.

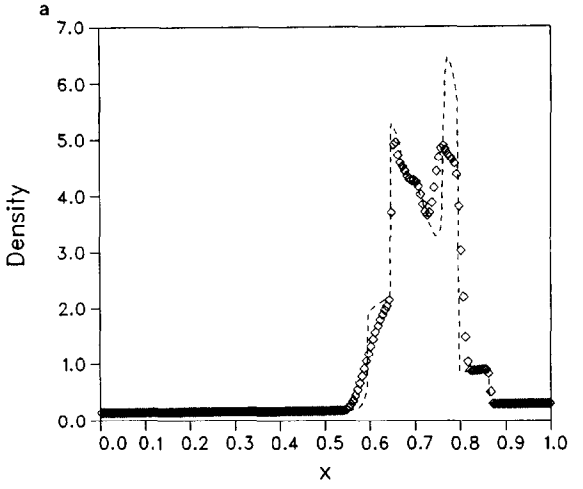

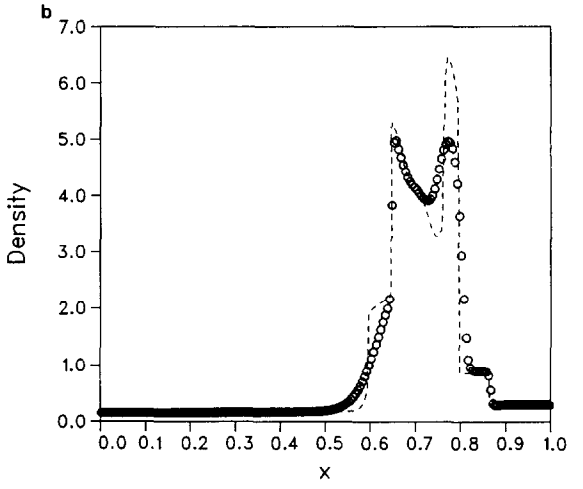

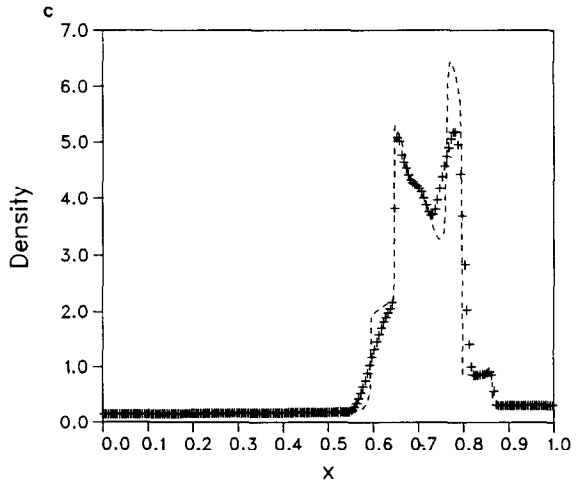

FIG. 5. Blast waves, Ref. [9], $t = 0.038$, $N = 200$, CFL = 0.2: (a) −, exact; ◇, TVD3; (b) −, exact; ○, UNO2; (c) −, exact; +, FNO3.

solution extrema between $x = 0.6$ and $x = 0.8$. It also gives the most accurate result at the slope discontinuity of density at around $x = 6.8$.

In conclusion, a fixed-stencil non-oscillatory upwind scheme based on the hybrid of a third-order five-point interpolation and a second-order non-oscillatory limiter has been constructed and tested in a series of calculations. The extension to a system of equations is verified by a shock tube problem and the interaction of blast waves. The scheme shows a higher accuracy than the conventional TVD3 and UNO2 scheme. The trade-off is about 10% of CPU time for the one-dimensional Euler solutions presented here. This new scheme seems well suited for problems with both smooth extrema and sharp discontinuities present in the solution, for example, in a supersonic mixing problem.

REFERENCES

1. A. Harten, *J. Comput. Phys.* **49**, 357 (1983).
2. S. R. Chakravarthy and S. Osher, *Lectures in Applied Mathematics*, Vol. 22 (Amer. Math. Soc., Providence, RI, 1985), p. 57.
3. W. K. Anderson, J. L. Thomas, and B. Van Leer, *AIAA J.* **24**, 1453 (1986).
4. H. C. Yee and A. Harten, *AIAA J.* **25**, 266 (1987).
5. A. Jameson, *Communications on Pure and Applied Mathematics*, Vol. XLI (Wiley, New York, 1988), p. 507.
6. A. Harten and S. Osher, *SIAM J. Numer. Anal.* **24**, 279 (1987).
7. A. Harten and S. Osher, *J. Comput. Phys.* **71**, 231 (1987).
8. B. Van Leer, *J. Comput. Phys.* **32**, 101 (1979).
9. P. Woodward and P. Colella, *J. Comput. Phys.* **54**, 115 (1984).
10. S. I. Lin, Institute of Aeronautics and Astronautics, National Cheng Kung University, Tainan, Taiwan, ROC, private communication (1990).

Received April 23, 1990; revised March 5, 1991

DARTZI PAN
S. C. LEE
Institute of Aeronautics and Astronautics
National Cheng Kung University
Tainan, Taiwan
Republic of China